Journal of NeuroVirology (1997) 3, 401–416

http://www.jneurovirol.com

An analysis of HIV-1-associated inflammatory products in brain tissue of humans and SCID mice with HIV-1 encephalitis

Yuri Persidsky,[1,3] Manuel Buttini[4], Jenae Limoges[1,3], Paul Bock[1,3] and Howard E Gendelman[1,2,3]

Departments of [1]Pathology and Microbiology, [2]Medicine, Eppley Institute for Research in Cancer and Allied Diseases, [3]Center for Neurovirology and Neurodegenerative Disorders, University of Nebraska Medical Center, Omaha, Nebraska 68198-5215; and the [4]Gladstone Molecular Neurobiology Program and the Department of Neurology, University of California, San Francisco, California 94141-9100, USA

The human immunodeficiency virus type 1 (HIV)-associated dementia complex (ADC) is a neuroimmunological disorder fueled by viral replication in mononuclear phagocytes (MP) (brain macrophages and microglia). The elucidation of MP inflammatory factors involved in neurological dysfunction is pivotal for unraveling pathogenic mechanisms and in developing new therapies for this disease. Recent advances in animal model systems for ADC and its associated encephalitis have provided important insights into how virus-infected macrophages cause brain injury. Indeed, the stereotactic inoculation of HIV infected monocytes into the basal ganglia/cortex of mice with severe combined immunodeficiency disease (SCID) results in pathological features similar to those of human HIV-1 encephalitis (HIVE). We used this SCID model to study the roles of macrophage secretory factors in HIVE. The expression of interleukin-1 (IL-1β, IL-6, IL-10), tumor necrosis factor-alpha (TNFα), vascular endothelial growth factor (VEGF), and adhesion molecules (E-selectin, intracellular cell adhesion molecule (ICAM-1), and vascular cell adhesion molecule-1 (VCAM-1)) in encephalitic brains of mice and humans was evaluated by semi-quantitative polymerase chain reaction (PCR). In SCID mice with HIVE, human and mouse TNFα, and mouse IL-6, VEGF, VCAM-1 and E-selectin were expressed at high levels. These results paralleled, to a great extent, those in HIVE brain tissues. Laser scanning confocal microscopy performed to assess the associated neuronal damage showed that microtubule associated protein-2 (MAP-2) immunoreactive dendrites were significantly reduced in both the ipsilateral and contralateral hemispheres of encephalitic mice. These results demonstrate the importance of macrophage inflammatory products in the pathogenesis of HIVE and further validates this model of viral encephalitis in SCID mice.

Keywords: animal model; inflammatory products; HIV encephalitis; neurotoxins; neuronal damage

Introduction

Primary infection of the brain with human immunodeficiency virus type 1 (HIV) is the most frequent cause of central nervous system (CNS) morbidity in people with the acquired immunodeficiency syndrome (AIDS) (Navia *et al*, 1986a,b). Up to 90% of AIDS patients have pathological changes in the brain at death (Navia *et al.*, 1986a,b). Clinical neurological manifestations of HIV infection collectively referred to as the HIV-associated dementia complex (ADC) occur in 15–20% of patients (Anders *et al*, 1986; Navia *et al*, 1986a; Price *et al*, 1988a,b) usually during advanced immunosuppression. The early stage of ADC is characterized by cognitive, motor, and behavioural impairments (Navia *et al*, 1986a). In later stages, the majority of patients develop global cognitive dysfunction which typically progresses to confusion, delusions, visual hallucinations, seizures, coma, and death (Navia *et al*, 1986a; Price *et al*, 1988a; Kieburtz and Schiffer, 1989; Parisi *et al*, 1991; Brew *et al*, 1995).

HIV infection of the CNS is manifested pathologically by the infiltration of virus-infected macro-

Correspondence: Howard E Gendelman, Director, Center for Neurovirology and Neurodegenerative Disorders, University of Nebraska Medical Center, 600 S 42nd Street, PO Box 985215; Omaha, NE 68198-5215, USA
Received 22 January 1997; revised 9 October 1997; accepted 14 October 1997

phages and the presence of multinucleated giant cells in the brain called HIV-1 encephalitis (HIVE) (Sharer *et al*, 1985; Budka, 1986; Koenig *et al*, 1986). Pathological abnormalities, including immunoreactive HIV infected brain macrophages/microglia, gliosis, myelin pallor and microglial nodules, are most prominent in the white and deep gray matter (especially the caudate and putamen) (Navia *et al*, 1986b; Petito *et al*, 1986; Wiley *et al*, 1986). In AIDS brains evaluated at autopsy, there is commonly diffuse myelin pallor and reactive astrocytosis (Navia *et al*, 1986b). Although most patients with HIV dementia have HIVE (Wiley and Achim, 1994; Glass *et al*, 1993), the two are not always associated (Brew *et al*, 1995). The underlying CNS abnormality that accounts for clinical neurological deficits is neuronal injury (including loss of synaptic contacts and dendrite alterations). Loss of neuronal subpopulations is most significant in the neocortex and deep grey matter (Masliah *et al*, 1992a,b).

Despite a clear clinical definition of ADC (Brew *et al*, 1995) and despite the relationship of ADC to brain macrophage infiltration, the pathogenesis of the disease remains uncertain. Although a number of factors have been identified during the last decade, including the role of neurotoxic products secreted by virus-infected and immune-activated mononuclear phagocytes (MP) (brain macrophages and microglia) (Genis *et al*, 1992; Tyor *et al*, 1992; Wesselingh *et al*, 1993; Griffin *et al*, 1994; Glass *et al*, 1993; Lipton and Gendelman, 1995; Nottet *et al*, 1995; Gendelman *et al*, 1997), the importance of neurotropic strains of HIV (Power *et al*, 1994; Korber *et al*, 1994), and the damaging effects of viral proteins on neurons (Lipton, 1992; Toggas *et al*, 1994; Weeks *et al*, 1995; Koka *et al*, 1995; Wyss-Coray *et al*, 1996), no consensus theory has emerged.

Relevant *in vivo* models were designed to test pathogenic mechanisms of ADC and to develop therapeutic interventions. To these ends, our laboratory recently developed a small animal model for HIV encephalitis (Persidsky *et al*, 1996). Severe combined immunodeficiency mice (SCID), mice stereotactically inoculated with HIV-infected monocytes into basal ganglia/cortex produced the salient features of HIV encephalitis astrogliosis, microglial nodules, MP activation, and neuronal death in response to relatively small numbers of virus-infected monocytes.

To analyze the utility of this mouse model for ADC in this study, we investigated the role of viral proteins, cytokines and other immune potentially neurotoxic products in HIVE. Analysis of human and mouse inflammatory factors in affected brain tissue showed similarities between the inflammatory responses of humans and SCID mice with HIVE. Importantly, the presence of HIV infected monocytes correlated with neuronal injury. These findings support the idea that HIVE is a metabolic encephalopathy caused by viral and host immune neurotoxins from macrophages and fueled by viral replication.

Results

Neuropathological features of HIVE in humans

To analyze the morphologic and molecular similarities between HIVE in humans and in SCID mice we first evaluated postmortem brain tissue from four patients with HIVE, two who died of opportunistic infectious complications but without neurological impairments, and three who died of causes not related to HIV infection (Table 1). In humans with HIVE the pathological features included the presence of multinucleated giant cells (MGC), perivascular macrophages, microglial nodules and astrogliosis (Figure 1a,c,e,g). MGC and macrophage brain infiltration were identified in the deep white matter of the cerebral hemispheres and in the basal ganglia. These cells expressed HLA-DR and HIV-1 p24 antigens (Figure 1c,g). In some instances the MGC had long cell processes, which suggested that the fused macrophages had arisen from, or had incorporated microglia (Figure 1a,c). Focal degeneration of white matter was associated with pallor, astrogliosis, and vacuolation. Macrophages containing myelin debris were readily observed. Rare foci

Table 1 Clinical and morphological findings in nine patients from postmortem brain tissue

Case	*Age (years)*	*AIDS**	*HIVE*	*Clinical and neuropathological diagnosis*
1	37	+	+	HIVE/progressive dementia
2	39	+	+	HIVE/progressive dementia
3	35	+	+	HIVE/progressive dementia/*Pneumocystis carinii* pneumonia
4	12	+	+	HIVE/progressive dementia
5	42	+	−	Disseminated intravascular coagulation/multiorgan failure
6	64	+	−	Generalized cachexia/malignant B cell lymphoma
7	61	−	−	Multiple sclerosis
8	71	−	−	Squamous cell carcinoma of lung
9	51	−	−	Hepatocellular carcinoma/altered mental status

*AIDS (Center for Disease Control and Prevention case definition of HIV-seropositive subject with $CD4^+$ T lymphocytes < 200 mm^3). HIVE, HIV-1 encephalitis.

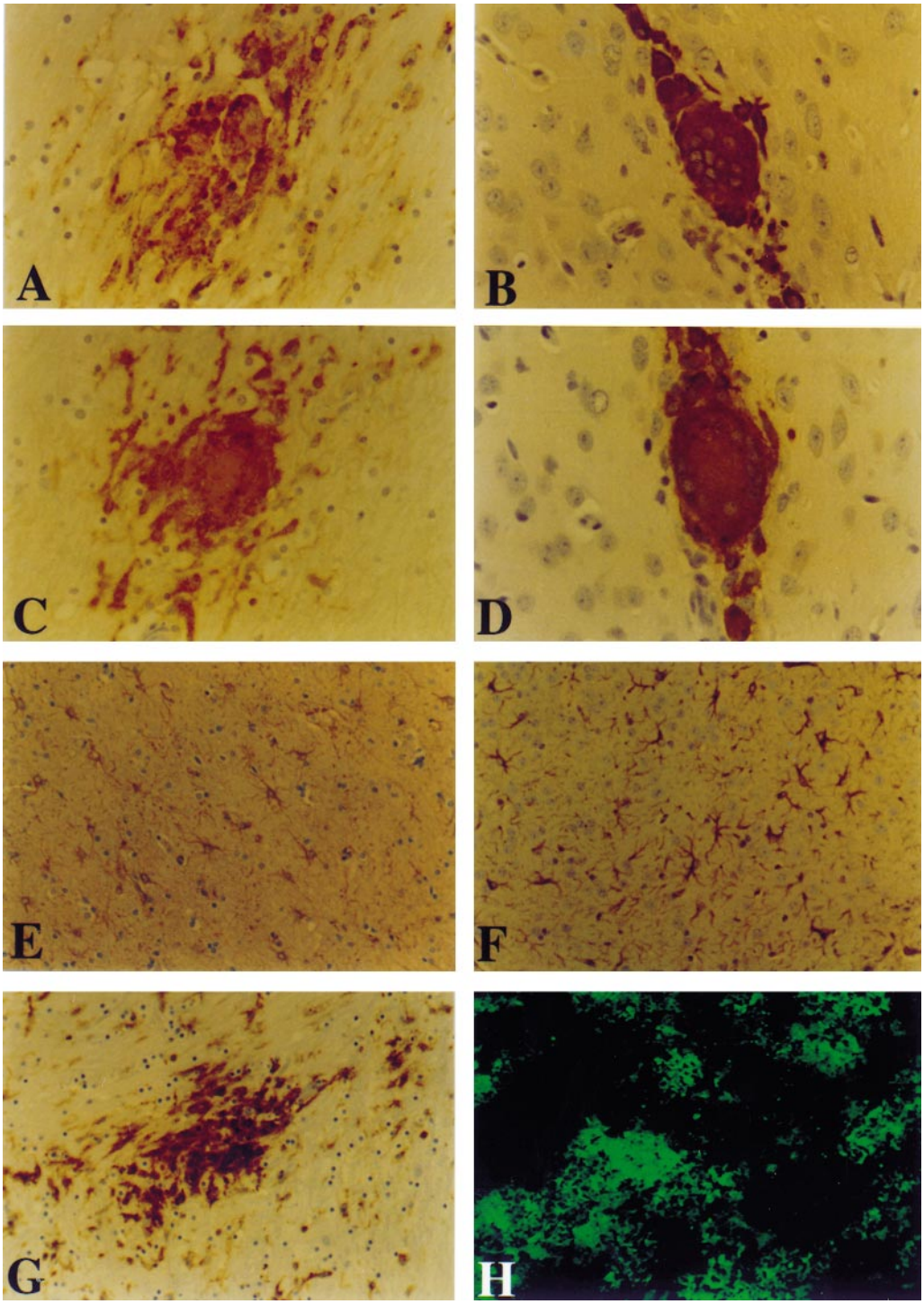

Figure 1 Morphological features of HIV encephalitis in human brain tissue (**A, C, E, G**) and in SCID mouse brain (**B, D, F, H**). Multi- and single nucleated CD68-positive cells were present in basal ganglia (**A, B**). Most expressed HIV-1 p24 antigen (**C, D**). Pronounced and widely spread astrogliosis was detected by anti-GFAP immunostaining in areas containing HIV-1 infected cells (**E, F**). Activated human (**G**) and mouse microglia (**H**) formed nodules. **A, C, E, G** present serial sections of human brain, and panels **B, D, F, H** present serial coronal sections of SCID mouse brain immunostained with antibodies against CD68 (**A, B**), HIV-1 p24 antigen (**C, D**), GFAP (**E, F**), HLA-DR (**G**) or F4/80 (mouse macrophage antigen) (**H**). Primary antibodies were detected by Vectastain Elite Kit using diaminobenzidine (DAB) as a substrate. F4/80 was visualized by immunofluorescence assay. Tissue sections were counterstained with Mayer's hematoxylin. Original magnification: **A–D, G** and **H**, ×400; **E** and **F**, ×200.

of neuronal degeneration were seen in the middle layers of the cortex. Opportunistic infections of the brain were not found.

Neuropathological features of HIVE in SCID mice

The neuropathological features of HIVE described above were reproduced by stereotactic inoculation of human HIV-infected monocytes into the brains of SCID mice. Animals (three per group) were injected with HIV infected or control uninfected monocytes. For both the infected and control animals human monocytes were observed in mouse brain up to 5 weeks after injection, as demonstrated by immunostaining for CD68 antigen (Figure 1b) or vimentin (data not shown). Monocytes were found in the basal ganglia (putamen and globus pallidus) and cortex along the needle track. Some of the monocytes were localized around microvessels as in human HIVE. The number of human monocytes in mouse CNS decreased from an average of 60 per section 3–7 days after inoculation to an average of eight cells 5 weeks after manipulation. Infected monocytes were seen in equal numbers and distribution as the uninfected cells, but readily formed MGCs (Figure 1b,d) and expressed viral proteins. About 30% of the human monocytes expressed HIV-1 p24 antigen at 1 week after injection, and 80% were antigen positive at 5 weeks. HLA-DR antigen expression was detected in 70% of the inoculated human cells. A reactive astrogliosis which was initiated at 3 days, peaked at 7 days and persisted for 5 weeks afer monocyte placement. The intensity of the astroglial reaction correlated with the number of cells injected. Astrocytes around the injected human cells displayed thick processes, enhanced GFAP immunoreactivity and big 'empty' nuclei with chromatin condensation (Figure 1f). Few monocytes were demonstrated in the contralateral ventricle and meninges, and their presence provoked a widespread astrogliosis. Microglial nodules were first demonstrated 3 days after human monocyte inoculation and at 7 days had readily identifiable multiple branching processes. The nodules were F4/80-positive and clustered around human monocytes (Figure 1h). The size of microglia paralleled the degree of astrocytosis. Endothelial cells expressing vascular cell adhesion molecule (VCAM)-1 were largely in and around microvessels in mouse brains containing HIV infected monocytes. Intercellular adhesion molecule (ICAM)-1 antigen was minimally increased. The astrocyte and microglial reactions resulting from the needle trauma were localized and distinct from those in brains containing human monocytes (data not shown).

Neuronal damage identified in brains of SCID mice with HIVE

Neuronal damage is a central neuropathological feature of HIVE of humans (Masliah *et al*, 1992a,b). To determine if similar findings occur in SCID mice with HIVE we studied neuronal damage induced by monocytes inoculated into brain after 5 weeks by semi-quantitative microtubule associated protein (MAP)-2 immunohistochemistry and laser scanning confocal microscopy in combination with computer-aided image analysis (Table 2).

Neuronal damage, was shown by loss of dendritic processes on MAP-2-immunolabeled brain sections in the caudate/putamen and neocortex of animals inoculated with human monocytes (Figure 2). This neuronal damage was patchy. In some areas, the damage was moderate, in other areas, severe damage with substantial reduction in the number of MAP-2-immunoreactive dendrites was seen. Moderate neuronal damage was found most frequently in the ipsilateral hemibrains of mice inoculated with uninfected monocytes (Figure 2b) and in the contralateral hemibrains of mice inoculated with HIV infected monocytes (Figure 2d). Importantly, severe neuronal damage was found most frequently in the ipsilateral hemibrains of mice inoculated with HIV-1 infected monocytes (Figure 2c). After inoculation with uninfected monocytes, little or no neuronal damage was detected in the contralateral hemibrains (data not shown). The distribution of neuronal damage in the neocortex was similar to that in the caudate/putamen, some areas show extensive loss of dendritic processes (Figure 2f) and others show no apparent changes (data not shown).

Since the neuronal damage was observed more consistently in the caudate/putamen than in the neocortex, the caudate/putamen was chosen for

Table 2 Quantition of MAP-2 immunostaining in brains of SCID mice with HIVE

Treatment	*Animal*	*Mean neuropil area occupied by MAP-2 positive dendrites*	
		Ipsilateral	*Contralateral*
None	1	22.1±4.8	28.9±2.6
	2	27.4±0.6	24.7±3.0
	3	28.1±2.0	27.7±3.3
Sham	4	27.5±3.6	30.0±3.1
	5	26.0±3.7	28.0±2.9
Inoculation of uninfected monocytes	6	20.7±3.3	22.3±2.6
	7	22.9±2.5	22.9±3.7
	8	14.2±3.6	24.6±5.7
	9	17.0±3.0	20.9±6.1
Inoculation of HIV-1 infected monocytes	10	12.1±2.3	19.9±3.5
	11	15.3±4.7	18.2±4.3
	12	14.1±4.3	19.7±6.5
	13	13.9±4.8	20.3±5.0
	14	9.4±3.6	14.5±6.0
	15	8.0±1.1	12.6±2.7

Brain sections were analyzed immunohistochemically by laser confocal microscopy as described in Materials and methods. Values represent mean (±s.d.) of percent of neuropil occupied by MAP-2 immunoreactive dendrites for each animal assayed.

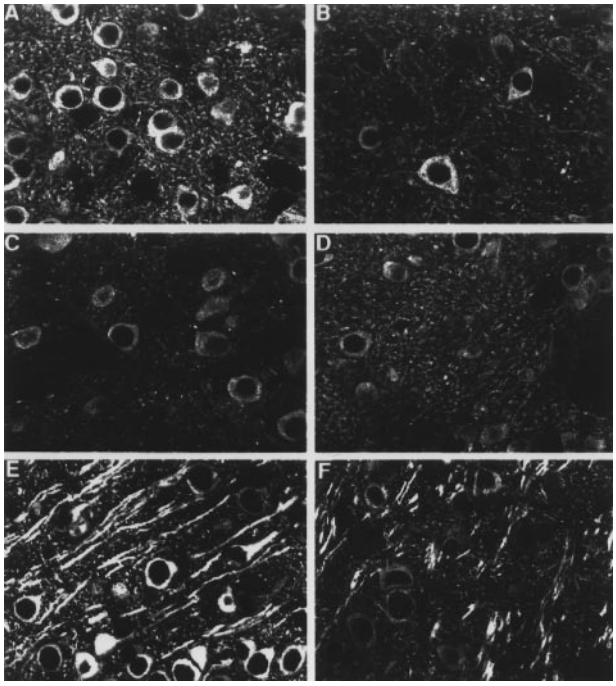

Figure 2 Loss of dendritic processes in the brains of SCID mice inoculated with uninfected (**B**) or HIV-1-infected (**C, D, F**) human monocytes revealed by confocal microscopy of brain sections immunolabeled with MAP-2. MAP-2 immunoreactivity was associated with neuronal cell bodies and dendrites in the caudate/putamen of a sham-inoculated mouse (**A**) and the neocortex of an unmanipulated mouse (**E**). Areas with moderate loss of dendritic processes are shown in **B** (ipsilateral caudate/putamen, uninfected monocytes) and **D** (contralateral caudate/putamen, HIV-infected monocytes). Areas with severe loss of dendritic processes are shown in **C** (ipsilateral caudate/putamen, HIV-infected monocytes) and **F** (ipsilateral neocortex, HIV-infected monocytes). Original magnification, ×400 for all panels.

semi-quantitative analysis of dendritic loss as described in Materials and methods (Table 2). Both HIV-infected and uninfected monocytes induced neuronal damage in the ipsilateral hemibrains (Figure 3, left panel), but only the infected monocytes induced significant neuronal damage in the contralateral hemibrains (Figure 3, right panel). Notably, dendritic loss was significantly more severe in brains of mice inoculated with HIV-1 -infected monocytes than in brains of mice inocuated with uninfected monocytes (Figure 3). Since the mice were inoculated with similar numbers of infected or uninfected cells, the more severe dendritic loss seen in the virus-infected monocyte animals is probably due either directly or indirectly to HIV infection.

Inflammatory products in human brains

To further substantiate the notion that the neuropathological features of HIVE in humans can be produced in SCID mice we undertook an extensive evaluation of the inflammatory products produced in human brains during HIV encephalitis. Initial experiments used semi-quantitative RNA polymerase chain reaction (PCR) assays to detect proinflammatory cytokines in different regions (cortex, basal ganglia, white matter, cerebellum) of encephalitic and control brains (Table 1). The primers used for these and subsequent experiments are shown in Tables 3 and 4. The results are summarized in Table 5 and Figure 4.

Because the number of macrophages in brain can reflect the severity of ADC (Glass *et al*., 1993) we first assessed the level of CD14 expression (a marker for MP cells) in encephalitic and control brain tissues (Table 5 and Figure 4). Increased CD14 mRNA levels were uniformly higher in patients with HIVE than in controls. These results reflected the distribution of macrophages demonstrated by CD68 or HAM 56 immunostaining (data not shown). Importantly, CD14 mRNA levels correlated significantly with tumor necrosis factor alpha (TNFα) expression, but not interleukin-1 (IL-1β), HIV-1*pol* or other cytokines, adhesion molecules or metalloproteinases. HIV-1*pol* mRNA was observed in all brain regions with morphological signs of encephalitis (Table 5, Figure 4). In control brains without encephalitis HIV-1*pol* was absent.

TNFα mRNA levels were higher in all HIV infected brain tissues than in controls (Table 5). TNFα levels were highest in HIVE brains (Figure 4). TNFα expression correlated significantly with that of IL-1β, IL-6, E-selectin, and VCAM-1. No correlations between TNFα, HIV-1*pol* or glial fibrillary acidic protein (GFAP) expression were found. IL-1β levels were statistically higher in HIV-1 infected patients. Interestingly, IL-1β expression correlated with ICAM-1 levels. IL-6 mRNA levels were not higher in HIV-1 infected patients. Interestingly, IL-1β expression correlated with ICAM-1 levels. IL-6 mRNA levels were not higher in HIV-1 infected patients.

Comparison of expression of two adhesion molecules (E-selectin and VCAM-1) in the brain tissue of patients with HIV-1 encephalitis and controls failed to reach statistical significance. VCAM-1 and E-selectin RNAs correlated well with each other and with TNFα. CD14 levels did not correlate with adhesion molecule expression suggesting that the upregulation of adhesion molecules does not necessarily correlate with the numbers of brain macrophages. ICAM-1 was upregulated in nonencephalitic tissue but lower in brains with HIVE. Vascular endothelial growth factor (VEGF) expression was similar, in all brains examined, regardless of whether HIVE was present. There was no relationship between VEGF expression and encephalitis. However, VEGF did correlate with GFAP.

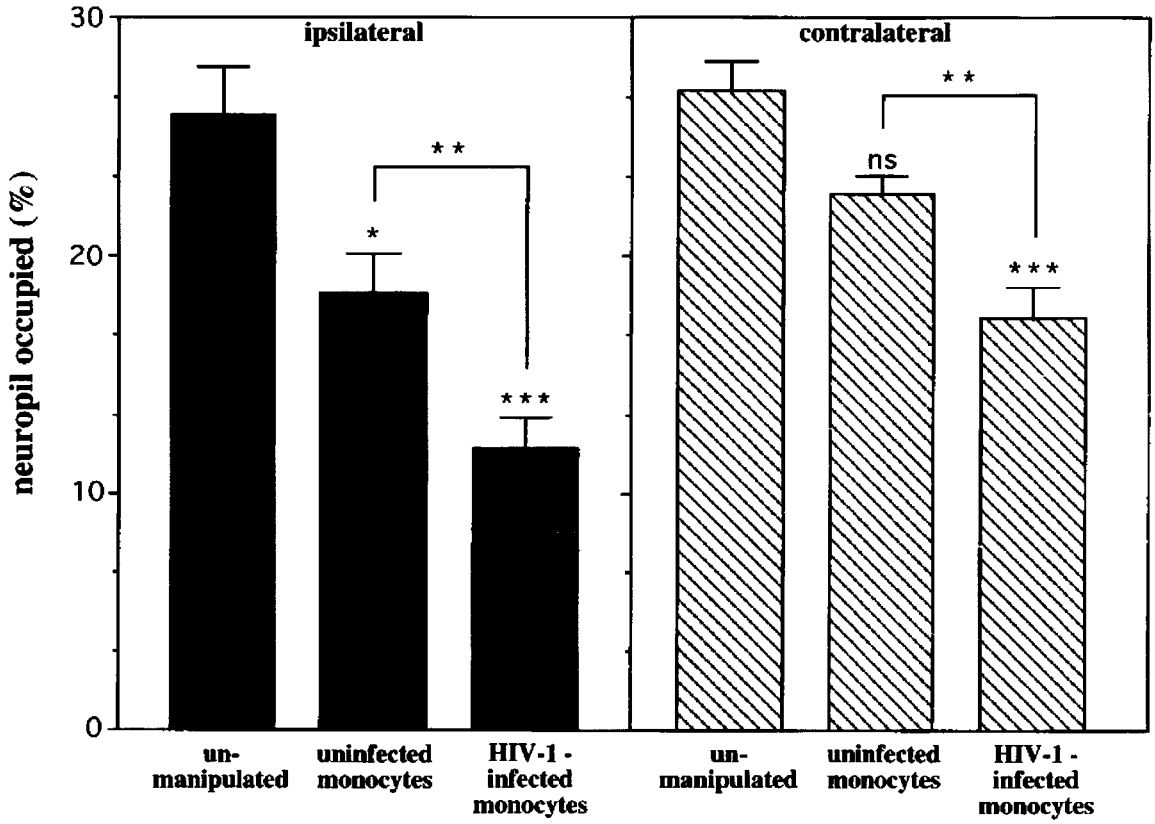

Figure 3 Neurodegeneration induced by HIV-infected and uninfected human monocytes in the ipsilateral and contralateral caudate/putamen of SCID mice. Laser scanning confocal images of MAP-2-immunolabeled brain sections from SCID mice inoculated with HIV-infected (six mice) or uninfected (four mice) human monocytes were analyzed as described in Materials and methods. Unmanipulated (three mice) and sham-inoculated (two mice, not shown), SCID mice served as controls. Values are the mean $\pm$ s.e.m. of the percent area of the neuropil occupied by MAP-2-immunoreactive dendrites. The values obtained for the brains of the two sham-inoculated animals (27.5% and 26% for the ipsilateral hemispheres, 30% and 28% for the contralateral hemispheres) were similar to the values obtained for unmanipulated mice (average of 25.9% for the ipsilateral hemisphere and of 26.9% for the contralateral hemisphere). MAP-2 immunoreactive dendrites were significantly reduced in both hemispheres of mice inoculated with HIV-infected monocytes and in the ipsilateral hemisphere of mice inoculated with uninfected monocytes. In both hemispheres, the damage induced by HIV-infected monocytes was significantly more severe than the damage induced by uninfected monocytes. $^{*}P<0.05$; $^{**}P<0.02$; $^{***}P<0.01$; ns, not significant.

Human inflammatory products in SCID mouse brains

HIV-infected or uninfected monocytes were stereotactically inoculated (ten SCID mice each) into the left hemisphere of the brain. After 1 week the animals were sacrificed and RNA extracted from the whole hemisphere of the inoculated and noninjected area. RNA–PCR assays were performed to assay differences between viral, cell and inflammatory factors in HIV-1 infected and control monocyte containing brains. Differences between inoculated and noninjected hemispheres were also assessed (see below). The results of these experiments are shown in Figure 5 and Table 6.

To evaluate secretory products of the human monocytes placed into the SCID brains, we first confirmed the monocytes presence by analyzing the levels of human CD14 (Figure 5). CD14 is a marker for human monocytes and its mRNA was found in the injected hemispheres of animals inoculated with control (uninfected) human cells (Table 6). CD14 mRNAs were also observed in the contralateral (noninjected) hemispheres demonstrating that the uninfected human monocytes can migrate (by whatever mechanism(s)) into the opposite hemisphere. CD14 mRNA levels were, surprisingly, not uniformly detected in brains inoculated with virus-infected monocytes. This could be related to a downregulation of CD14 as a result of HIV infection or to lower numbers of HIV infected cells that migrated through the subarachnoid space or brain parenchyma. The findings may also reflect, in measure, virus-induced cell death, or to MGCs in the HIV-1 cell preparations rendering the cells less able to migrate from the inoculated site from the syringe placement. In support of the former, a $>30\%$ downregulation of CD14 expression was found in cultured HIV-1 infected monocytes than in uninfected controls (data not shown).

Table 3 Oligonucleotide primers used in RNA–PCR assays for human products

Amplification product (size)	*Nucleotide position*	*Primer*	*Sequence*
Nested CD14 (527 bp)	719–740	sense	TCTCTGTCCCCACAAGTTCCCC
Nested CD14 (527 bp)	1226–1244	antisense	GCCAAGGCAGTTTGAGTCC
CD14 (268 bp)	881–907	sense	ATGCATGTGGTCCAGCGCCC
	1135–1153	antisense	CCACCGACAGGGTCGAACG
	963–982	probe	AGCCAAGCTCAGAGTGCTCG
TNFα (237 bp)	503–527	sense	GAGCTGAGAGATAACCAGCTGGTG
	740–716	antisense	CAGATAGATGGGCTCATACCAGGG
	588–608	probe	CCCTCCACCCATGTGCTCCTC
IL-1β (179 bp)	480–500	sense	AAAAGCTTGGTGATGTCTGG
	659–638	antisense	TTTCAACACGCAGGACAGG
	549–567	probe	ATGGAGCAACAAGTGGTG
IL-6 (159 bp)	317–357	sense	GTGTGAAAGCAGCAAAGAGGC
	476–455	antisense	CTGGAGGTACTCTAGGTATAC
	399–420	probe	GGATTCAATGAGGAGACTTGC
IL-10 (265 bp)	128–148	sense	GATCTCCGAGATGCCTTCAGC
	393–373	antisense	GGAAGAAATCGATGACAGCGC
	244–263	probe	AGCCTTGTCTGAGATGATCC
VCAM-1 (281 bp)	234–253	sense	TCTCATTGACTTGCAGCACC
	515–495	antisense	ACTTGACTGTGATCGGCTTCC
	372–391	probe	ACGAACACTCTTACCTGTGC
E-Selectin (257 bp)	612–640	sense	TACACTTGCAAGTGTGACCC
	878–857	antisense	TGTCACAGCATCACACTCAACC
	669–690	probe	ATTGTGAACTGTACAGCCCTGG
ICAM-1 (287 bp)	334–353	sense	TATTCAAACTGCCCTGATGG
	621–601	antisense	TAGTGCGGCACGAGAAATTGG
	367–390	probe	AAAACCTTCCTCACCGTGTACTGG
VEGF (153 bp)	152–171	sense	AGGAGGGCAGAATCATCACG
	283–302	antisense	TCGCATCAGGGGCACACAGG
	273–292	probe	GGCACACAGGATGACTTGAA
GADPH	199–217	sense	CCATGGAGAAGGCTGGGG
	394–374	antisense	CAAAGTTGTCATGGATGACC
	280–299	probe	CTGCACCACCAACTGCTTAGC

To confirm the presence of HIV infected monocytes in mouse brains by the PCR assays we designed nested primers for CD14. The nested RNA–PCR showed CD14 mRNA in all animals inoculated with HIV-1 infected monocytes. All mouse brains inoculated with virus-infected monocytes had detectable HIV-1*pol*. HIV-1*pol* did not correlate with inflammatory molecule expression. This suggests that the level of viral infection does not necessarily correlate with cytokine levels or that the infected cells preferentially produce more TNFα per cell, but the same amount or less IL-10 and IL-6.

Human TNFα was significantly higher (more than twofold) in mouse brains inoculated with HIV infected monocytes as compared to uninfected controls (Table 6, Figure 5). Both the infected and the contralateral hemisphere had high levels of TNFα. This suggested that TNFα could be readily detected despite the reduced number of human cells. CD14 and TNFα RNA expression correlated.

Modest decreases in human IL-10 and IL-6 were detected in mouse brains with virus-infected monocytes as compared to controls. Such differences were likely related to their decreased production in infected monocytes. CD14 and IL-6 levels correlated with each other but not with IL-10. IL-1β, IL-8, and TGFβ were not detected in mouse brains inoculated with HIV infected or control monocytes.

Mouse inflammatory products in SCID mouse brains

In these experiments, a variety of inflammatory products including TNFα, IL-1β, IL-6, VEGF, the inducible form of nitric oxide synthase (iNOS), E-selectin, ICAM-1 and VCAM-1 were analyzed in SCID mice inoculated with HIV infected monocytes and in control mice inoculated with uninfected monocytes or with media alone. The findings are shown in Table 7 and Figure 5. Mouse TNFα, IL-6, VEGF, and VCAM-1 levels were all higher in mouse brains containing HIV infected monocytes than in controls. Although TNFα levels were 1.7 times higher in brains with HIV infected than uninfected monocyte brains the differences were not significant (Table 7) (Figure 5). Differences between TNFα mRNA between injected monocytes in both hemispheres were significant for encephalitic mice only. IL-6 mRNA levels were fourfold higher in mice with HIV infected monocytes than in animals inoculated with control cells. Mouse VEGF was 2.3-fold

Table 4 Oligonucleotide primers used in RNA–PCR assays for mouse products

Amplification product (size)	*Nucleotide position*	*Primer*	*Sequence*
TNFα (200 bp)	124–143	sense	CTCCCTCCAGAAAAGACACC
	302–321	antisense	TTTGGGGACCGATCACCCCG
	154–174	probe	AAAGCATGATCCGCGACGTGG
IL-1β (242 bp)	157–176	sense	GACCCCAAAAGATGAAGGGC
	377–396	antisense	ATGAGTCACAGAGGATGGGC
	203–222	probe	TCCAGATGAGAGCATCCAGC
IL-6 (157 bp)	127–146	sense	ACTTCACAAGTCCGGAGAGG
	262–251	antisense	TTCATACAATCAGAATTGCC
	160–179	probe	GATACCACTCCCAACAGACC
IL-10 (180 bp)	881–900	sense	ACTTTATAGTATTTAAAGGG
	1039–1058	antisense	TTCTTCACAACTCTCTTAGG
	931–950	probe	CCTTGGGAAGCAATTGAAGC
VCAM-1 (255 bp)	734–753	sense	GGGATGTACAGAGATCGTCG
	501–521	antisense	GGAGATTGATCTGTTCAAGGG
	599–619	probe	CCTTTACTCCCGTCATTGAGG
E-selectin (223 bp)	821–840	sense	GCAGGCGCACTCCACTCTCC
	620–640	antisense	ACCTGCAAGTGCCACCCTGGC
	714–733	probe	GCTCCCACCCGTTCGGCCCC
ICAM-1β (346 bp)	204–224	sense	CTTCCTCATGCAAGGAGGACC
	528–547	antisense	CCCACCCACTGGCTGGCGGC
	420–439	probe	CAGCCTGGCAGCAAGTAGGC
VEGF (250 bp)	176–195	sense	AGAAGGAGAGCAGAAGTCCC
	404–423	antisense	TTTGGTGAGGTTTGATCCGC
	254–273	probe	CCTGGTGGACATCTTCCAGG
GFAP (212 bp)	1458–1477	sense	CCCCAGCTGGTTAGAATTGG
	1648–1667	antisense	TGGCATTCGTGATGCATAGG
	1563–1582	probe	TGGAAGTTTCCACAGGCTGC
iNOS (191 bp)	384–404	sense	CCTAAGAGTCACCAAAATGG
	554–573	antisense	GGACTTGCAAGTGAAATCCG
	476–495	probe	CCCGTCCACAGTATGTGAGG

higher in mouse brains inoculated with HIV-infected monocytes than in those inoculated with control monocytes (Table 7). Significant differences were shown between the injected and contralateral hemispheres. Similar results were observed for mouse VCAM-1. VCAM-1 was constitutively expressed in mouse brain tissue (Figure 5). Nonetheless, VCAM-1 levels were twofold higher in brain tissues inoculated with HIV-1 infected monocytes than in the contralateral hemisphere or in tissues inoculated with control uninfected monocytes (Table 7). Similarly, E-selectin mRNA was nearly twofold higher in HIV-infected mouse brains (for both inoculated and contralateral hemispheres) than in brains inoculated with uninfected monocytes. Mouse ICAM-1 was increased at statistically significant levels only in brains inoculated with control uninfected monocytes. VCAM-1 correlated with E-selectin and ICAM-1 but only in mice inoculated with HIV infected monocytes. iNOS RNA was increased in all monocyte inoculated brains but did not reach statistical significance. IL-1β mRNA levels in brains inoculated with HIV infected monocytes as compared to controls failed to reach statistical significance. IL-10 levels showed no significant differences between HIV-1 monocyte or controls. Mouse TNFα levels correlated with mouse IL-6, IL-1β, and GFAP in brain tissues containing infected or uninfected monocytes. Interestingly, VCAM-1 and iNOS correlated with mouse TNFα only in the mice inoculated with HIV infected monocytes. Human CD14 correlated with mouse TNFα, GFAP, ICAM-1, and IL-1β expression. HIV-1*pol* correlated with mouse TNFα and VCAM-1 in SCID mice injected with virus-infected cells. Human TNFα correlated with mouse TNFα in all monocytes inoculated brains.

GFAP expression was higher in hemispheres inoculated with HIV-infected monocytes or uninfected monocytes as compared to the contralateral noninjected hemispheres. GFAP levels were higher in brains inoculated with infected monocytes. These differences did not, however, reach significance (Table 7). Human TNFα correlated with GFAP. GFAP correlated with VCAM-1 and iNOS in brain tissue with HIV infected monocytes.

These results, taken together with the previous neuropathological analyses strongly support the relevance of the SCID mouse model of HIV encephalitis to human disease. Most importantly, the results demonstrate that such inflammatory

effects are most likely mediated by virus-infected macrophages.

Discussion

The present study demonstrates that neuronal injury and inflammatory factors in human HIV encephalitis can be produced in a SCID mouse. Inoculation with HIV-infected monocytes upregulated a number of inflammatory factors including TNFα, IL-6, VEGF, VCAM-1, and E-selectin, in the brains of SCID mice. These products also showed associations one with another. Interestingly, IL-1β, a cytokine not associated with human HIV encephalitis, was found at higher levels in mouse brains inoculated with control uninfected monocytes. GFAP expression was only minimally upregulated in brains with HIV-1 encephalitis than in human and mouse suggesting that the changes found at the protein level likely occur at a posttranscriptional level. Similar patterns of cytokine regulation were observed in human and mouse brains with HIV-1 encephalitis including the upregulation of both human TNFα and mouse TNFα, VCAM-1, and E selectin; the absence of statistically significant correlation between HIV-1*pol* and the expression of inflammatory factors, and the capacity of virus-infected macrophages to induce a significant inflammatory reaction in brain tissue. Taken together these findings support the notion that the SCID mouse model of HIV encephalitis is relevant for mirroring aspects of the human disease.

The few differences in inflammatory factor expression between human and mouse brain tissues (for example IL-6, VEGF) could be related to the trauma of cell inoculation or altered responses of different mammalian species to virus and/or cytokine production. These could affect the complex regulation of inflammatory products by human or mouse cells. Moreover, the elevated levels of cytokines and other proinflammatory products in the peripheral blood of HIV-infected patients may also affect the expression of inflammatory factors in brain. No experiments that could generate such similarities were attempted in this study. Nevertheless, similarities between the expression of a variety of inflammatory factors in human and mouse brains were shown clearly and reproducibly. Importantly, these data show that inflammatory neurotoxins produced by human monocytes can

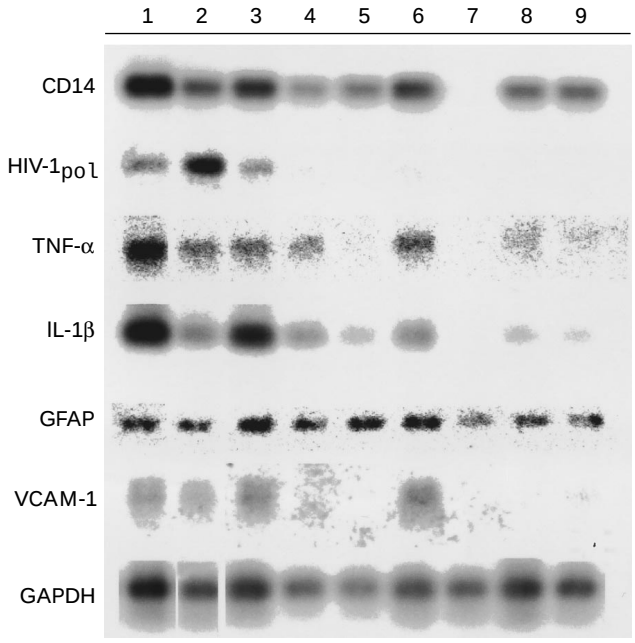

Figure 4 Expression of mRNA for CD14, HIV-1*pol*, TNFα,IL-1β, GFAP, VCAM-1 in human brains affected by HIV-1 encephalitis/HIV-1 associated dementia (cases 1, 2, 3, and 4), HIV positive patients without signs of encephalitis (cases 5 and 6), and seronegative controls (cases 7, 8, and 9). RNA was reverse transcribed and then amplified by PCR for 28 cycles. Coupled reverse transcription/PCR amplification products were visualized by Southern blot hybridization. The mRNA for the cellular enzyme glyceraldehyde 3-phosphate dehydrogenase (GAPDH) served as an internal control to allow analysis and comparison of RNA species between different samples using a Molecular Dynamic's PhosphorImager 425B.

Table 5 RNA–PCR analysis of viral and cellular monocytes secretions in human brains with HIVE

Viral and cellular products	*HIVE brains*	*Non-encephalitic brains*		P *values*		
		HIV seropositive	*HIV seronegative*	*A*	*B*	*C*
CD14	32±5.7	15±6	10±6	<0.05	NA	NA
HIV-1 *pol*	2.82±1.14	0	0	NA*	0.0099	NA
TNFα	272±82	140±52	17±6.7	<0.05	NS	<0.02
IL-1β	27±4.4	17±0.3	6±0.6	NS	NS	<0.004
IL-6	76±11.4	136±4.50	42±5.4	NS	NS	0.05
VCAM-1	101±10.8	85±4.5	33±3.3	NS	<0.03	NS
ICAM-1	130±18.2	405±83.7	47±8.8	<0.01	NS	<0.03

NS, not significant: NA, not applicable. Levels of RNA isolated from 5 different brain regions were quantitated after cDNA amplication for 28 cycles. Comparisons between species of RNA were made utilizing a ratio to GAPDH (mean±s.e.m.$\times 10^3$) as an internal control and quantitation of the amplified products with a phosphorimager. A=HIV-1 encephalitic versus non-encephalitic brains; B=HIV-1 encephalitic versus HIV seronegative brains; C=non-encephalitic versus HIV nonencephalitic brains.

Table 6 RNA–PCR analysis of human monocyte secretory products in mouse brain tissue

Human cytokines	*Unifected monocytes*		*HIV-1-infected monocytes*		P *values*		
	Ipsilateral	*Contralateral*	*Ipsilateral*	*Contralateral*	*A*	*B*	*C*
CD14	26±4	6±0.6	0*	0*	<0.0001	NA	NA
HIV-*pol*	0	0	172±57	5±1	NA	0.0099	NA
TNF-α	25±4	14±2	52±10[#]	33±6	<0.03	NS	<0.02
IL-6	66±9	21±7	28±11	22±14	<0.002	NS	<0.004
IL-10	13±1	9±2	8±2	6±2	NS	NS	0.05
MMP-1	20±1	20±3	24±3	14±2	NS	<0.03	NS
MMP-9	11±3	1±0.3	3±0.4	2±0.3	<0.02	NS	<0.03

*Presence of monocytes was verified by nested PCR for CD14. NA, not applicable; NS, not significant. Levels of RNA were quantitated after cDNA amplification for 28 cycles. Comparisons between species of RNA were made utilizing a ratio to GAPDH (mean ± s.e.m. × 10^3) as an internal control and quantitation of the amplified products with a Phosphorimager. *P* values are shown (right) between brains where control uninfected monocytes were inoculated (A) and compared to the non-inoculated contralateral hemisphere; (B) the HIV-1 infected monocytes inoculated hemisphere compared to the non-inoculated contralateral hemisphere and (C) HIV-1 inoculated as compared to control monocyte-injected brain hemisphere.

affect neuroimmune activities in mouse brain tissue. The results further provide an explanation for the neuropathological changes (including microglial nodule formation, astrogliosis, and neuronal injury) demonstrated in the SCID mouse brains inoculated with HIV-infected monocytes (Persidsky *et al*, 1996). These changes are likely mediated by immunological factors secreted in response to viral infection and immune activation of brain macrophages and microglia. These secretory activities could affect both the autocrine and paracrine production of cytokines in the affected brains of humans and mice.

Levels of CD14 RNA served as an important indicator for monocyte brain infiltration in both animals inoculated with HIV-1 infected and control uninfected cells. The inability to detect CD14 gene expression in brains of animals inoculated with virus-infected monocytes could reflect a down-regulation of CD14 within the infected monocytes and/or decreased ability of the infected monocytes to migrate from the areas of inoculation. Indeed, the MGCs may have less ability to move within the affected hemisphere or to cross hemispheres. This could be related to cell death or defects in migratory function as related to cell size or viral infection. This explains, in measure, the apparent discrepancy between the histopathological data, which showed equal numbers of virus infected and control monocytes in immunostained tissues, and the RNA–PCR results which showed decreased levels of CD14 RNA in the brains inoculated with infected as compared to uninfected monocytes.

The central feature of HIV encephalitis is neuronal damage. Neuronal injury resembling that in humans with ADC was elicited in the brains of SCID mice by human monocytes. The area occupied by MAP-2-immunoreactive dendrites was significantly reduced in both the ipsilateral and contralateral hemibrain of mice inoculated with HIV-infected monocytes and in the ipsilateral hemibrains of mice inoculated with uninfected monocytes. Virus-infected monocytes induced significantly more pronounced neuronal injury than uninfected monocytes. Such dendritic damage and reduction were previously found distinct in humans with HIV-1 encephalitis (Masliah *et al*, 1992a).

This study also demonstrates that HIV-infected monocytes can induce inflammatory reactions in brain that affect neurotoxic activities. Therefore, these cells may be key effectors of neuronal damage in the brains of HIV-1-infected patients. The neurotoxic properties of human monocytes could be explained by several, possibly synergistic, mechanisms. Implantation of purified human monocytes into mouse brain activates the cells and induces the production of neurotoxins (Persidsky *et al*, 1996), which may be increased by HIV infection. HIV infection primes monocytes for activation (Gendelman *et al*, 1997) and, as a consequence, stimulated virus-infected monocytes may produce a variety of potential neurotoxins in greater abundance than stimulated uninfected cells. In the brains of SCID mice inoculated with human monocytes, autocrine stimulation of the implanted monocytes by monocyte-derived factors, as well as paracrine stimulation by factors of endogenous mouse brain cells, such as proinflammatory cytokines expressed by microglia (Persidsky *et al*, 1996), may all contribute to the persistent activation of the implanted monocytes. This hypothesis is supported by the upregulation of several distinct inflammatory factors, produced in large measure by activated macrophages and proposed to play central roles in neurotoxic responses in affected brains with HIV-1 encephalitis.

Potentially noxious molecules produced by activated monocytes include inflammatory cytokines, such as TNFα and IL-1β (Genis *et al*, 1992; Merrill and Martinez-Maza, 1993; Nottet *et al*, 1995), eicosanoids (Genis *et al*, 1992; Nottet *et al*,

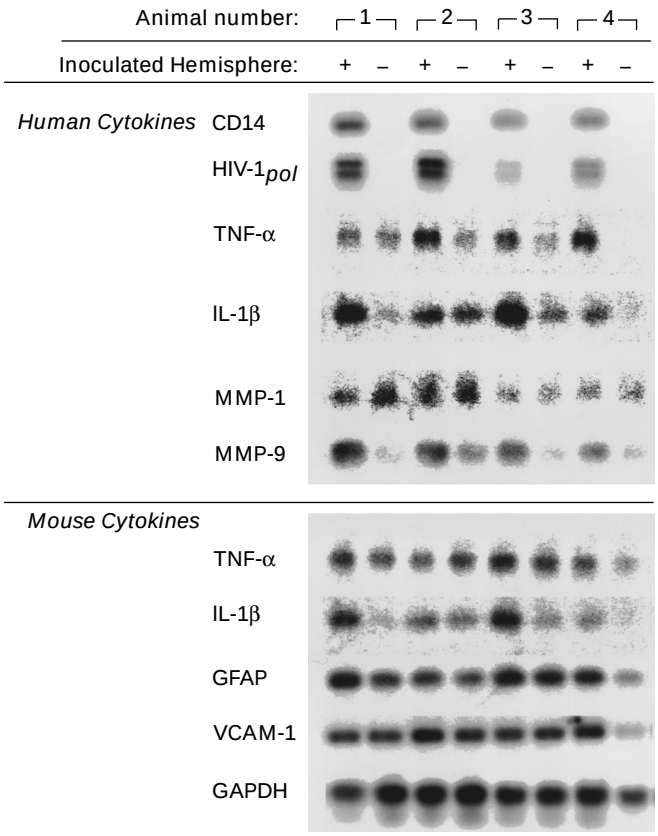

Figure 5 Detection of mRNA for human and mouse proinflammatory products in the SCID mouse brains with HIV encephalitis. SCID mice were stereotactically inoculated with 1×10^5 HIV infected (ten animals) or uninfected monocytes (ten animals). Mice were sacrificed 1 week after inoculation, and RNA was extracted from injected and contralateral (unmanipulated) hemispheres. The results are shown for four mice inoculated with HIV infected monocytes (inoculated hemispheres labeled with '+') and are represented for all animals investigated. Oligonucleotide primers for specific human (CD14, HIV-1*pol*, TNFα, IL-1β, MMP-1 and -9) and mouse products (TNFα, IL-1β, GFAP, VCAM-1) were designed from sequences obtained from Genbank. mRNA for mouse cytokines did not cross-react with analogous human cytokine mRNAs. RNA was reverse transcribed and then amplified by PCR for 28 cycles. Coupled reverse transcription/PCR amplification products were visualized by Southern blot hybridization. The mRNA for the cellular enzyme glyceraldehyde 3-phosphate dehydrogenase (GAPDH) served as an internal control to allow analysis and comparison of RNA species between different samples using a Molecular Dynamic's PhosphorImager 425B.

1995), free radicals (Piani *et al*, 1992; Dawson *et al*, 1993; Bukrinsky *et al*, 1995), platelet-activating factor (Gelbard *et al*, 1994), and excitotoxic amino acids (Piani *et al*, 1992; Lipton, 1992; Lipton and Rosenberg, 1994). In addition, secretion of HIV-1 proteins such as gp120, gp41 and tat, which have been shown to induce neuronal injury *in vivo* (Mucke *et al*, 1995; Wyss-Coray *et al*, 1996; Weeks *et al*, 1995; Adamson *et al*, 1996), may contribute to the neurotoxicity caused by HIV-infected monocytes (Wahl *et al*, 1989; Lipton, 1992; Guilian *et al*, 1993). The combined action of endogenous monocyte products, HIV factors, and secretions derived from mouse cells likely accounts for the dramatic neuronal damage observed in the brains of mice inoculated with infected monocytes.

The findings of this study may also support *in vivo* evaluations of therapeutic compounds aimed at preventing neuronal injury or reducing macrophage inflammatory responses that affect neuronal impairments in HIV-infected patients. Substances such as glutamate receptor antagonists, anti-inflammatory compounds, or free radical scavengers may all help limit the neuronal damage caused by activated MPs. For example, the N-methyl-D-aspartate receptor antagonist memantine prevent neuronal injury in the brains of gp120 transgenic mice (Toggas *et al*, 1996), and the antiinflammatory compound and phosphodiesterase inhibitor pentoxifylline suppresses TNFα transcription (Chao *et al*., 1993). TNFα may affect neuronal viability as well as stimulate HIV replication in monocytes (Poli *et al*, 1990) and microglia (Peterson *et al*, 1992). Since TNFα is strongly suspected to contribute to neuronal damage in the brains of HIV-infected patients (Merrill and Martinez-Maza, 1993), suppression of TNFα secretion may limit monocyte-mediated neuronal injury.

In summary, we have demonstrated that HIV-infected monocytes in the brains of SCID mice elicit pronounced inflammatory responses resulting in neuronal damage. These results suggest that HIV infection primes macrophages for activation and lead to increased secretion of neurotoxins and increased neuronal injury associated with HIV infection. Such effects could be limited by therapies that target HIV replication, prevent the production of inflammatory factors from activated MP, inhibit monocyte transendothelial migration into the brain, or protect neurons from neurotoxic activities. These results further substantiate the relevance of the SCID mouse model to the neuropathogenesis of HIV-1 infection and the importance of macrophages in disease.

Materials and methods

Isolation and culture of primary human monocytes
Monocytes were recovered from PBMC's of HIV and hepatitis B seronegative donors after leukopheresis, and were purified by counter current centrifugal elutriation. Cell suspensions were >98% monocytes by criteria of cell morphology and Wright-stained cytosmears, by granular peroxidase, by nonspecific esterase, and CD68 labeling (monocyte-macrophage marker). Monocytes were cultured in Teflon flasks (2×10^6 cells/ml, 150×10^6 cells/flask) in Dulbecco's modified Eagle's media (DMEM) (Sigma, St. Louis, MO) with 10% heat-inactivated pooled human serum, 50 μg/ml genta-

Table 7 RNA PCR analysis of mouse monocyte secretory products in the brains of SCID mice with HIV encephalitis

	Uninfected monocytes		*HIV-1-infected monocytes*		*P values*		
Mouse Cytokines	*Ipsilateral*	*Contralateral*	*Ipsilateral*	*Contralateral*	*A*	*B*	*C*
TNF-α	42 ± 5	31 ± 4	74 ± 15	41 ± 8	<0.04	NS	NS
IL-1β	35 ± 8	16 ± 3	23 ± 6	17 ± 3	<0.04	NS	NS
IL-6	5 ± 1	6 ± 2	21 ± 5	18 ± 7	NS	NS	<0.03
VEGF	58 ± 12	46 ± 8	136 ± 29	111 ± 15	NS	NS	<0.05
VCAM-1	129 ± 14	126 ± 17	225 ± 33	115 ± 26	NS	<0.02	<0.02
E Selectin	11 ± 1	14 ± 2	28 ± 9	22 ± 6	NS	NS	NS
GFAP	143 ± 16	86 ± 6	180 ± 30	103 ± 15	<0.004	<0.05	NS

NS, not significant. Levels of RNA were quantitated after cDNA amplification for 28 cycles. Comparisons between species of RNA were made utilizing a ratio to GAPDH (mean $\pm$ s.e.m. $\times 10^3$) as an internal control and quantitation of the amplified products with a Phosphorimager. *P* values are shown (right) between brains where control uninfected monocytes were inoculated (A) and compared to the non-inoculated contralateral hemisphere; (B) the HIV-1 infected monocytes inoculated hemispere compared to the non-inoculated contralateral hemisphere and (C) HIV-1 inoculated as compared to control monocyte-injected brain hemisphere.

micin (Sigma), 10 μg/ml ciprofloxacin (Sigma Chemical Co.), and 1000 U/ml highly purified recombinant humanmacrophage CSF (a generous gift from Genetics Institute Inc., Cambridge, MA) (Kalter *et al*, 1991). All tissue culture reagents were screened before use and found negative for endotoxin (<10 pg/ml; Associates of Cape Cod, Woods Hole, MA) and mycoplasma contamination (Gen-probe II; Gen-probe, San Diego, CA).

HIV infection of monocytes

After 7 days in suspension, cultured monocytes were infected with HIV-1_{ADA} at multiplicity of infection (MOI) of one infectious viral particle/target cell (Gendelman *et al*, 1988). The culture medium was exchanged every 3 days. Reverse transcriptase (RT) activity was determined in triplicate samples of culture fluids added to a reaction mixture of 0.05% Nonidet P-40 (Sigma), 10 μg/ml poly(A), 0.25 μg/ml oligo(dt) (Pharmacia Fine Chemicals, Piscataway, NJ), 5 mM DTT (Pharmacia), 150 mM KCl, 15 mM $MgCl_2$, and [^{3}H]dTTP (2 Ci/mmol; Amersham, Arlington Heights, IL) in pH 7.9 Tris-HCl buffer for 24 h at 37°C. Radio labeled nucleotides were precipitated with cold 10% TCA and 95% ethanol in automatic cell harvester (Skatron, Sterling, VA) on paper filters. Radioactivity was estimated by liquid scintillation spectroscopy. The percentage of HIV-1 p24 monoclonal antibody (Dako, Carpenteria, CA). Cytospin preparations of HIV-1 infected or noninfected cells were fixed in cold absolute acetone/methanol (1 : 1) for 10 min at -20°C, and then anti-p24 monoclonal antibody (Dako, 1 : 10) was applied for 45 min at room temperature, followed by treatment with FITC-conjugated anti-mouse IgG, F(ab′)$_2$ fragment (Boehringer Mannheim Corp., Indianapolis, IN; 1 : 100). Viral antigen-positive cells were counted with FITC-filter in a Nikon Microphot-FXA microscope (Nikon, Tokyo, Japan) using a $\times 20$ objective in ten random fields. All experiments were performed in triplicate.

SCID mouse model

The SCID mice (male C.B-17/IcrCrl-*SCID-bg*BR 3–4 weeks old) were purchased from Charles River Laboratories (Wilmington, MA). Animals were maintained in sterile microisolator cages under pathogen-free conditions in the Laboratory of Animal Medicine at the University of Nebraska Medical Center (UNMC) in accordance with ethical guidelines for care of laboratory animals set forth by the National Institutes of Health. All animal manipulations (including intracranial inoculations) were made in a laminar flow hood. Intracerebral injections of HIV-1_{ADA}-infected or control uninfected monocytes were performed following intraperitoneal (i.p.) ketamine/xylazine anesthesia (100 mg/kg ketamine and 16 mg/kg xylazine). On the day of brain inoculation (day 7 post infection) cells were pelleted. A monocyte suspension of 2×10^7 cells/ml was prepared for injections. SCID mice were anesthetized and placed in a stereotaxic apparatus (Stoetling Co., Wood Dale, IL) designed specifically for mice. The animal's head, following anesthesia, was secured with earbars and mouthpiece. Each animal was inoculated with 15 μl of suspension containing 2×10^5 cells. The coordinates for the inoculation (putamen) were: 3.5 mm behind the bregma, 3.5 mm lateral from the sagittal midline at a depth and angle of 4.0 mm and 35° from vertical line respectively with 100 μl Hamilton syringe and a 26 guage needle. This technique of intracerebral inoculation was reproducible in multiple separate experiments. Animals were sacrificed 1 week after intracerebral inoculation. Ten mice were inoculated in each of three conditions: human monocytes, HIV-1-infected human monocytes, and DMEM culture media (sham) inoculum. At 7 days post-inoculation all mice were sacrificed, and the whole brain was collected. The brain stem was removed, the hemispheres separated, and RNA was extracted from each hemisphere individually.

Immunohistochemistry
Brain tissue was collected at necropsy and frozen in OCT compound in cassettes for cryostat sectioning. Six coronal blocks (about 1 mm in thickness) were prepared from each brain, and ten sections (6 μm) were cut from each block and double immunostained for GFAP (astrocytosis) and CD68 or vimentin (monocyte distribution). Additional serial sections were obtained from the block containing the inoculation site (usually block 3), 30 and from the immediately adjacent blocks (u = ten sections per block). Monocytes were identified in mouse brain tissue by morphological and immunohistochemical assays in each study.

Immunohistochemistry was performed on 6 μm thick cryostat sections fixed in absolute acetone/methanol (1 : 1) for 10 min at -20°C. Human monocyte-derived macrophages were identified with anti-CD68 KP-1 (Dako, 1 : 100) or anti-vimentin (Boehringer Mannheim, Indianapolis, IN; 1 : 25) monoclonal antibodies. Mouse astrocytes were recognized with polyclonal antibodies against glial fibrillary acidic protein (GFAP) (Dako 1 : 100). Mouse microglia/macrophages were identified with rat monoclonal antibody F4/80 (Serotech, Kidlington, UK). Mouse VCAM-1 was identified with rat mAb (PharMingen, San Diego, CA) at a 1 : 25 dilution). Mouse ICAM-1 was detected with hamster mAb (PharMingen and used at 1 : 50 dilution). Human HLA-DR (Boehringer Mannheim 1 : 25) and HIV p24 antigens (Dako 1 : 10) mAbs were used to detect macrophage activation and HIV-1 protein expression respectively.

Indirect immunofluorescence detection (secondary Abs) was performed with FITC-coupled anti-mouse IgG, $F(ab')_2$ fragment, or anti-rabbit Abs IgG, $F(ab')_2$ fragment (Boehringer Mannheim 1 : 100) labeled with rhodamine. Goat anti-rat Ab, $F(ab')_2$ fragment (Biosource) coupled with FITC was used as the detection step for the primary rat mAbs. Immunostained tissues were analyzed with a Nikon Microphot-FXA microscope. Double labeling (with anti-CD68 and anti GFAP) was done on replicate tissue sections to characterize astrocyte reactions to human monocytes. Absence of the primary antibody or use of mouse IgG or rabbit IgG (Dako) served as controls. To detect antigens (CD68, HLA-DR, HIV-1, p24, GFAP, vimentin, NSE, MAP-2, neurofilaments and PGP 9.5) on paraffin sections, avidin-biotin immunoperoxidase staining Vectastain Elite ABC kit (Vector Laboratories, Burlingame, CA) was used with 3,3′-diaminobenzidine as the chromogen. Then sections were counterstained with Mayer's hematoxylin.

Tissue preparation for laser confocal microscopy
For laser confocal microscopic analysis of neuronal damage, mice inoculated with uninfected monocytes (n=4) HIV-infected monocytes (n=6) or medium only unmanipulated controls (n=4) were anesthetized and perfused transcardially with 0.9% saline five weeks after implantation of the monocytes. The brains were removed and postfixed for 48 h in 4% paraformaldehyde in phosphate-buffered saline (PBS: 2.6 mM KCl, 1.4 mM KH_2PO_4, 136 mM NaCl, 8 mM Na_2HPO_4). Vibratome sections (40 μm) were prepared and stored in cryoprotectant medium (0.1 M phosphate buffer containing 30% glycerin and 30% ethylene glycol) at -20°C until use. Brains of additional animals were removed 1 week (n=6) and 5 weeks (n=2) after monocyte implantation to prepare frozen or paraffin-embedded coronal sections covering a distance of about 600 μm (rostrally and caudally) from the injection site. These sections were used to confirm the presence of human monocytes and of HIV by immunostaining with anti-CD68 and anti-p24 antibodies, respectively. Primary antibody binding was detected by the avidin-biotin immunoperoxidase technique (Vectastain Elite ABC kit; Vector Laboratories, Burlingame, CA), and sections were counterstained with Mayer's hematoxylin.

Laser confocal microscopy
Two vibratome brain sections at the level of the caudate/putamen (near the inoculation site of human monocytes) per animal were immunolabeled with an antibody directed against MAP-2, a marker for neuronal dendrites, and then incubated with a FITC-labeled secondary antibody. For each mouse, (six to nine different laser scanning confocal images for the caudate/putamen of each hemibrain) covering a surface of 210×140 μm each, were obtained and analyzed, essentially as described (Masliah *et al*, 1992a), with a Bio-Rad MRC-1024 mounted on a Nikon Optiphot-2 microscope. Digitized images were transferred to a PowerMacintosh 8500 running a public domain program written by Wayne Rasband (NIH Image). The area of the neuropil occupied by MAP-2-immunolabeled dendrites was quantified and expressed as a percentage of the total image area, as described (Masliah *et al*, 1992a).

In view of the patchy distribution of neuronal damage after implantation of human monocytes and to obtain a representative value for loss of dendritic processes in each group of animals, four to six of the most severely affected areas and two to three less severely affected areas were imaged for each hemisphere in which neuronal damage was identified. For each control animal (unmanipulated and sham-inoculated mice), two or three images for the caudate/putamen of each hemibrain were analyzed. Values for individual hemibrains represent the mean of all the readings obtained from the different areas imaged.

Oligonucleotides for RNA–PCR assays
To analyze murine cytokine response to human macrophages, oligonucleotide primers for specific mouse cytokine mRNA were designed from mRNA

sequences obtained from Genbank. The computer program Amplify 1.2 was utilized to assess efficiency and reactivity of primer sequences. Only primers that produced one product of suitable size from mouse mRNA, and no product from analogous human mRNA, were used. To further test the reactivity of the primers, PCR against HIV-infected and uninfected human monocytes RNA, and total cellular RNA from mice brain tissue were analyzed. For controls, total cellular RNA from liver, spleen, and brain from control animals, and animals challenged with 50 μg and 100 μg of LPS, were also examined. Primers for human and mouse products used in this work are listed in Tables 2 and 3.

Isolation of total cellular RNA
Total cellular RNA was isolated from mouse or human brain tissue (see below) using TRIzol reagent (Life Technologies). Briefly, whole tissue was homogenized in 1 ml of TRIzol per 50–100 mg tissue, or cells were lysed by repetitive pipetting in 1 ml of TRIzol reagent per 50–100 million cells. RNA was extracted using chloroform, and precipitated with isopropanol. The samples were treated two times with 10 μl RNAse free RQ1 DNAse (1000 u/ml; from Promega). The DNA-free RNA was then precipitated using 3M sodium acetate and ethanol. To verify that DNA contamination was absent, a DNA–PCR for glyceraldehyde 3-phosphate dehydrogenase (GAPDH) was utilized.

RNA–PCR assay
Levels of cytokine RNA's were examined after reverse transcription with antisense primers and PCR amplification of cDNA transcripts. RNA from glyceraldehyde 3-phosphate dehydrogenase (GAPDH) served as an internal standard for quantitation utilizing a Molecular Dynamic's PhosphorImager 425B equalizing results to GAPDH cell expression for densitometric analysis.

One μg total cellular RNA in 5 μl was mixed with 0.5 μg of antisense primer (primer sequences are attached). The mixture was heated at 70°C for 10 min then cooled to 4°C. RT (Life Technologies, 200 U/μl) and 1.5 μl each of the four deoxynucleotide triphospates (10 mM, Perkin Elmer) were added. RT reactions were at 37°C for 15 min, and were stopped by heating the sample to 95°C. For PCR amplification of cDNA products, one-half of the mixture was discarded, then 0.5 μg sense and 0.25 μg antisense primers were added, with 1 μl each of the four deoxynucleotide triphosphates, and 0.5 μl Amplitaq DNA polymerase (5 U/μl, Perkin Elmer). Primer and probe sequences for human and mouse products are listed in Tables 2 and 3, respectively. A semi-quantitative RNA–PCR analysis was made of secretory products from human monocytes and mouse brain tissue. Amplified products (at the linear range of the assay) were quantitated utilizing ratios of product to GAPDH. The latter was used as an internal standard for all RNA–PCR products scored with a PhosphorImager 425B.

To increase the sensitivity of CD14 nested PCR was performed with primers were yielding a 527 bp product from CD14 RNA. After the initial amplification using the above-mentioned PCR method, 2.5 μl of cDNA was subjected to a second amplification using primers amplifying an interior portion of the 527 bp cDNA, and yielding a 268 bp product. 0.5 μg each of sense and antisense primers were mixed with the cDNA in the presence of 1 μl each of the four deoxynucleotide triphosphates, and 0.5 μl Amplitaq DNA polymerase (5 U/μl, Perkin Elmer). The products of 28 cycles (30 s, 94°C; 30 s, 50°C; 60 s, 72°C) were analyzed using Southern Blot hybridization, with ^{32}P-labeled oligonucleotides.

Brain autopsy materials
Brain tissue, derived from five separate regions, from 6 HIV-1 infected and three control cases (who were HIV-1 negative) was used for immunohistological assessment and total cellular RNA isolation. A concise description of clinical history pertaining to each of the brain samples is shown in Table 1. Immunohistochemical evaluation of macrophage infiltration and microglia reaction (anti-CD68 or HAM 56 mAbs), activation (HLA-DR expression), level of infection (HIV-1 p24 antigen), astrogliosis (GFAP) and expression of adhesion molecules (VCAM-1, E-selectin and ICAM-1) was performed on frozen tissue sections by indirect immunofluorescence and avidin-biotin immunoperoxidase staining Vectastain Elite ABC kit (Vector Laboratories, Burlingame, CA) as described above and before (Persidsky *et al*, 1996). Then, total RNA was isolated from the same tissue pieces used for immunohistological evaluation. This approach enabled us to compare levels of RNA for secretory products with tissue pathology. Amplified products (at the linear range of the assay) were quantitated utilizing ratios of product to GAPDH. The latter was used as an internal standard for all RNA–PCR products scored with a PhosphorImager 425B (as described above).

Statistical analyses
Differences between means of the results obtained for different products by RT–PCR and MAP-2 staining in the separate groups of mice were analyzed with a two-tailed Student's *t*-test. Differences among means were analyzed by one-way ANOVA with the different treatments as the independent factor, when significant differences were detected, pair-wise comparisons between means were evaluated by Dunnett's multiple comparison test. In all analyses, the null hypothesis was rejected at the 0.05 level.

Acknowledgements

We thank Dr E Masliah for helpful advice on laser scanning confocal microscopy and computer-aided analysis of confocal images and Dr Lennart Mucke for critical review of the manuscript. Ms Karen Spiegel's efforts are appreciated for excellent editorial and graphic assistance. This work was supported by National Institutes of Health grants RO1 NS36126-01 (HEG), PO1 MH57556-01 (HEG), PO1 NS31492-01 (HEG), RO1 NS 34239-01 (HEG), the University of Nebraska Medical Center start up funds and the Charles A Dana foundation (HEG). Jenae Limoges is a Nicholas Badami Fellow of the Department of Pathology and Microbiology, University of Nebraska Medical Center.

References

Adamson CD, Wildemann B, Sasaki M, Glass JD, McArthur JC, Christov VI, Dawson TM, Dawson VL (1996). Immunologic NO synthetase: Elevation in severe AIDS dementia and induction by HIV-1 gp41. *Science* **274:** 1917–1921.

Anders KH, Guerra WF, Tomiyasu U, Verity MA, Vinters HV (1986). The neuropathology of AIDS: UCLA experience and review. *Am J Pathol* **124:** 537–558.

Brew BJ, Rosenblum M, Cronin K, Price RW (1995). AIDS dementia complex and HIV-1 brain infection: Clinical-virological correlations. *Ann Neurol* **38:** 563–570.

Budka H (1986). Multinucleated giant cells in brain: a hallmark of the acquired immune deficiency syndrome (AIDS). *Acta Neuropathol (Berl)* **69:** 253–258.

Bukrinsky M, Nottet HSLM, Schmidtmayerova H, Dubrovsky L, Flanagan CR, Mullins ME, Lipton SA, Gendelman HE (1995). Regulation of nitric oxide synthase activity in human immunodeficiency virus type 1 (HIV-1)-infected monocytes: implications for HIV-associated neurological disease. *J Exp Med* **181:** 735–745.

Chao CC, Hu S, Close K, Choi CS, Molitor TW, Novick WJ and Peterson PK. (1992). Cytokine release by microglia: Differential inhibition by pentoxifylllin and dexamethasone. *J Inf Dis.* **166:** 847–853.

Dawson VL, Dawson TM, Uhl GR, Snyder SH (1993). Human immunodeficiency virus-1 coat protein neurotoxicity mediated by nitric oxide in primary cortical cultures. *Proc Natl Acad Sci USA* **90:** 3256–3259.

Gelbard HA, Nottet HSLM, Swindells S, Jett M, Dzenko KA, Genis P, White R, Wang L, Choi Y-B, Zhang D, Lipton SA, Tourtellotte WW, Epstein LG, Gendelman HE (1994). Platelet-activating factor: a candidate human immunodeficiency virus type 1-induced neurotoxin. *J Virol* **68:** 4628–4635.

Gendelman HE, Orenstein JM, Martin MA, Ferruca C, Mitra R, Phipps T, Wahl LA, Lane HC, Fauci SD, Burke DS, Skillman DR, Meltzer MS (1988). Efficient isolation and propagation of human immunodeficiency virus on recombinant colony-stimulating factor 1-treated monocytes. *J Exp Med* **167:** 1498–1506.

Gendelman HE, Persidsky Y, Ghorpade A, Limoges J, Stins M, Fiala M, Morrisett R (1997). The neuropathogenesis of HIV-1 dementia. *AIDS* **11 suppl. A):** S35–45.

Genis P, Jett M, Bernton EW, Boyle T, Gelbard HA, Dzenko K, Keane RW, Resnick L, Mizrachi Y, Volsky DJ, Epstein LG, Gendelman HE (1992). Cytokines and arachidonic metabolites produced during human immunodeficiency virus (HIV)-infected macrophage-astroglia interations: implications for the neuropathogenesis of HIV disease. *J Exp Med* **176:** 1703–1718.

Giulian D, Wendt E, Vaca K, Noonan CA (1993). The envelope glycoprotein of human immunodeficiency virus type 1 stimulates release of neurotoxins from monocytes. *Proc Natl Acad Sci USA* **90:** 2769–2773.

Glass JD, Wesselingh SL, Selnes OA, McArthur JC (1993). Clinical and neuropathologic correlation with HIV-associated dementia. *Ann Neurol* **33:** 2230–2237.

Griffin DE, Wesselingh SL, McArthur JC (1994). Elevated central nervous system prostaglandins in human immunodeficiency virus-associated dementia. *Ann Neurol* **35:** 592–599.

Kalter DC, Nakamura M, Turpin JA, Baca LM, Dieffenbach C, Ralph P, Gendelman HE, Meltzer MS (1991). Enhanced HIV replication in MCSF-treated monocytes. *J Immunol* **146:** 298–307.

Kieburtz K, Schiffer RB (1989). Neurological manifestations of human immunodeficiency virus infections. *Neurol Clin* **7:** 447–468.

Koenig S, Gendelman HE, Orenstein JM, Dal Canto MC, Pezeshkpour GH, Yungbluth M, Janotta F, Aksamit A, Martin MA, Fauci AS (1986). Detection of AIDS virus in macrophages in brain tissue from AIDS patients with encephalopathy. *Science* **233:** 1089–1093.

Koka P, He K, Zack JA, Kitchen S, Peacock W, Fried I, Tran T, Yashar SS, Marrill JE (1995). Human immunodeficiency virus 1 envelope proteins induce interleukin-1, tumor necrosis factor-α, and nitric oxide in glial cultures derived from fetal, neonatal and adult human brain. *J Exp Med* **182:** 941–952.

Korber BTM, Kunstman KJ, Patterson BK, Furtado M, McEvilly MM, Levy R, Wolinsky SM (1994). Genetic differences between blood- and brain-derived viral sequences from human immunodeficiency virus type-1 infected patients: Evidence of conserved elements in the V3 region of the envelope protein of brain-derived sequences. *J Virol* **68:** 7467–7481.

Lipton SA (1992). Requirement for macrophages in neuronal injury induced by HIV envelope protein gp120. *Neuroreport* **3:** 913–915.

Lipton SA (1994). Neuronal injury associated with HIV-1 and potential treatment with calcium-channel and NMDA antagonists. *Dev Neurosci* **16:** 145–151.

Lipton SA, Rosenberg RA (1994). Mechanisms of disease: Excitatory animo acids as final common pathway for neurological disorders. *N Engl J Med* **330:** 613–622.

Lipton SA, Gendelman HE (1995). Dementia associated with the acquired immunodeficiency syndrome. *N Engl J Med* **332:** 934–940.

Masliah E, Achim CL, Ge N, DeTeresa R, Terry RD, Wiley CA (1992a). Spectrum of human immunodeficiency virus-associated neocortical damage. *Ann Neurol* **32:** 321–329.

Masliah E, Ge N, Achim CL, Hansen LA, Wiley CA (1992b). Selective neuronal vulnerability in HIV encephalitis. *J Neuropathol Exp Neurol* **51:** 585–593.

Merrill JE, Martinez-Maza O (1993). Cytokines in AIDS-associated neurons and immune dysfunction. In: *Neurobiology of Cytokines. Methods in Neuroscience.* de Zouza EB (ed). Academic Press, San Diego: pp. 243–249.

Mucke L, Masliah E, Campbell IL (1995). Transgenic animal models to assess the neuropathogenic potential of HIV-1 proteins and cytokines. *Curr Top Microbiol Immunol* **202:** 187–205.

Navia BA, Jordan BD, Price RW (1986a). The AIDS dementia complex. I. Clinical features. *Ann Neurol* **19:** 517–524.

Navia BA, Cho E-S, Petito CK, Price RW (1986b). The AIDS dementia complex: II. Neuropathology. *Ann Neurol* **19:** 525–535.

Nottett HSLM, Jett M, Flanagan CR, Zhai Q-H, Persidsky Y, Rizzino A, Bernton EW, Genis P, Baldwin T, Schwartz J, LaBenz CJ, Gendelman HE (1995). A regulatory role for astrocytes in HIV-1 encephalitis: an overexpression of eicosanoids, platelet-activating factor, and tumor necrosis factor-α by activated HIV-1-infected monocytes is attenuated by primary human astrocytes. *J Immunol* **154:** 3567–3581.

Parisi A, Stossell M, Pan A, Maserati R, Minoli L (1991). HIV-related encephalitis presenting as convulsant disease. *Clin Electroenceph* **22:** 1–4.

Persidsky Y, Limoges J, McComb R, Bock P, Baldwin T, Tyor W, Patil A, Nottet HSM, Epstein L, Gelbard H, Flanagan E, Reinhard J, Pirruccello SJ, Gendelman HE (1996). Neuropathological analysis of HIV encephalitis in SCID mice. *Am J Pathol* **149:** 1027–1053.

Peterson PK, Gekker G, Hu S, Schoolov Y, Balfour HH, Chao CC (1992). Microglial cells upregulation of HIV-1 expression in the chronically infected promonocytic cell line U1: The role of tumor necrosis factor-α. *J Neuroimmunol* **14:** 81–88.

Petito CK, Cho E-S, Lemann W, Navia BA, Price RW (1986). Neuropathology of acquired immunodeficiency syndrome (AIDS): an autopsy review. *J Neuropathol Exp Neurol* **45:** 635–646.

Piani D, Spranger M, Frei K, Schaffner A, Fontana A (1992). Macrophage-induced cytotoxicity of N-methyl-D-Aspartate receptor positive neurons involves excitatory amino acids rather than reactive oxygen intermediates and cytokines. *Eur J Immunol* **22:** 2429–2436.

Poli G, Kinter A, Justement JS (1990). Tumor necrosis factor-a functions in an autocrine manner in the induction of human immunodeficiency virus expression. *Proc Natl Acad Sci USA* **87:** 782–785.

Power C, McArthur JC, Johnson RT, Griffin DE, Glass JD, Perryman S, Chesebro B (1994). Demented and nondemented patients with AIDS differ in brain-derived human immunodeficiency virus type 1 envelope sequences. *J Virol* **68:** 4643–4649.

Price RW, Brew B, Sidhs J, Rosenblum M, Sheck AC, Cleary P (1988a). The brain in AIDS: CNS HIV-1 infection and AIDS dementia complex. *Science* **239:** 586–592.

Price RW, Sidtis J, Rosenblum M (1988b). The AIDS dementia complex: some current questions. *Ann Neurol* **23:** S27–S33.

Sharer LR, Cho ES, Epstein LG (1985). Multinucleated giant cells and HTLV-III in AIDS encephalopathy. *Hum Pathol* **16:** 760.

Toggas SM, Masliah E, Rockenstein EM, Rall GF, Abraham CR, Mucke L (1994). Central nervous system damage produced by expression of the HIV-1 coat protein gp120 in transgenic mice. *Nature* **367:** 188–193.

Toggas SM, Masliah E, Mucke L (1996). Prevention of HIV-1 gp120-induced neuronal damage in the central nervous system of transgenic mice by the NMDA receptor antagonist memantine. *Brain Res* **706:** 303–307.

Tyor WR, Glass JD, Griffin JW, Becker PS, McArthur JC, Bezman L, Griffin DE (1992). Cytokine expression in the brain during the acquired immunodeficiency disease syndrome. *Ann Neurol* **31:** 349–360.

Wahl LM, Corcoran ML, Pyle SW, Arthur LO, Harel-Bellan A, Farrar WL (1989). Human immunodeficiency virus glycoprotein (gp120) induction of monocyte arachidonic acid metabolites and interleukin-1. *Proc Natl Acad Sci USA* **86:** 621–625.

Weeks BS, Lieberman DM, Johnson B (1995). Neurotoxicity of the human immunodeficiency virus type 1 tat transactivator to PC12 cells requires the tat amino acid 49–58 basic domain. *J Neurosc Res* **42:** 34–40.

Wesselingh SL, Power C, Glass JD, Tylor WR, McArthur JC, Farber JM, Griffin JW, Griffin DE (1993). Intracerebral cytokine mRNA expression in AIDS. *Ann Neurol* **33:** 576–582.

Wiley CA, Schrier RD, Nelson JA, Lampert PW, Oldstone MBA (1986). Cellular localization of human immunodeficiency virus infection within brains of acquired immune deficiency syndrome patients. *Proc Natl Acad Sci USA* **83:** 7089–7093.

Wiley CA, Achim C (1994). Human immunodeficiency virus encephalitis is the pathological correlate of dementia in acquired immunodeficiency disease syndrome. *Ann Neurol* **36:** 673–676.

Wyss-Coray T, Masliah E, Toggas S (1996). Dysregulation of signal transduction pathways as a potential mechanism of nervous system alterations in HIV-1 gp120 transgenic mice and humans with HIV-1 encephalitis. *J Clin Invest* **97:** 789–798.